Bull. Chem. Soc. Jpn. Vol. 80, No. 12, 2375–2377 (2007)

Spin-Crossover Behavior of Isomorphous Bi- and Mononuclear Iron(III) Complexes

Shinya Imatomi, Tetsuya Sato, Takefumi Hamamatsu, Ryoko Kitashima, and Naohide Matsumoto*

Department of Chemistry, Faculty of Science, Kumamoto University, 2-39-1 Kurokami, Kumamoto 860-8555

Received July 26, 2007; E-mail: naohide@aster.sci.kumamoto-u.ac.jp

Isomorphous bi- and mononuclear iron(III) complexes, $[Fe^{III}_2L_2(bimb)](BPh_4)_2$ (**1**) and $[Fe^{III}L(meim)]BPh_4$ (**2**), where H_2L = bis(3-methoxysalicylideneaminopropyl)amine, bimb = 1,4-bisimidazolylbutane, meim = *N*-methylimidazole, and BPh_4^- = tetraphenylborate, respectively, were synthsized. Binuclear complex **1** showed a two-step spin-crossover (SCO) behavior at $T_{1/2} = 60$ and 90 K, whereas mononuclear complex **2** showed a one-step SCO behavior at $T_{1/2} = 215$ K. The different SCO behavior can be ascribed to the quasi-one-dimensional structure constructed by π–π stacking and the binuclear structure.

The spin-crossover (SCO) phenomenon is one of the most fascinating electro-structural properties in coordination chemistry.[1] Because of the theoretical and experimental aspects, as well as the potential applications to new electronic devices. SCO complexes have attracted intense interest over the past decades.[1,2] Although the SCO behavior is essentially the phenomenon of a single molecule, it has been well recognized that the interaction between SCO sites is an important factor that governs the SCO properties, such as hysteresis and LIESST (Light-Induced Excited Spin State Trapping) effect.[1,3] The SCO behaviors are influenced complicatedly by many factors so that it is difficult to clarify the detailed SCO mechanism. Therefore, a simple model compound is needed in order to investigate each effect on the SCO properties. In our previous studies, we have synthesized a family of SCO iron(III) complexes with Schiff-base multidentate ligands derived from salicylaldehyde derivatives and linear polyamines, consisting of mononuclear, binuclear, and one-dimensional complexes,[4,5] in order to determine (1) how the ligand field strength of Schiff-base ligand can be tuned in the SCO region and (2) how the binuclear or one-dimensional structure affects on the SCO behavior. In the course of our study, we have found a pair of SCO complexes, $[Fe^{III}_2L_2(bimb)](BPh_4)_2$ (**1**) and $[Fe^{III}L(meim)]BPh_4$ (**2**), of which the crystal structures are isomorphous to each other and their magnetic properties show different SCO behaviors. Here, we report their synthesis, structure, and SCO behavior and discuss why these two complexes show different SCO behaviors.

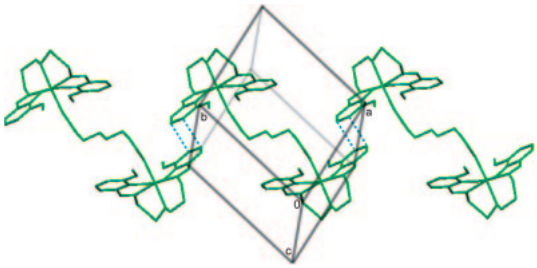

Fig. 1. Packing diagram of **1** at 296 K. BPh_4^- ions are omitted for clarity. Blue broken lines show π–π interaction.

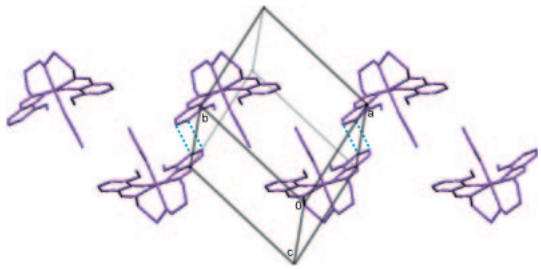

Fig. 2. Packing diagram of 2 at 296 K. BPh_4^- ions are omitted for clarity. Blue broken lines show π–π interaction.

Binuclear complex **1** was synthesized by mixing the precursor complex $[Fe^{III}ClL]$, 1,4-bisimidazolylbutane and sodium tetraphenylborate in a 2:1:2 mole ratio in methanol at room temperature and obtained as black block crystals. Mononuclear complex **2** was synthesized by mixing $[Fe^{III}ClL]$, *N*-methylimidazole, and sodium tetraphenylborate in a 1:1:1 mole ratio in methanol at room temperature. The two complexes showed thermochromism in the solid states from purple at room temperature to green at liquid nitrogen temperature, indicating SCO behavior.

The crystal structures of the two complexes were determined by single-crystal X-ray diffraction at 296 K.[4] The packing diagrams for the bi- and mononuclear complexes are shown in Figs. 1 and 2, respectively. As demonstrated by their crystallographic data, these two complexes crystallize in the same crystal system and the same space group, $P\bar{1}$ (No. 2) with very similar cell dimensions, in which binuclear complex **1** has an inversion center and the crystallographic unique unit is one half of a binuclear structure. Further, as evidenced by the tables of the atomic coordinates and packing diagrams, the corresponding atomic coordinate of bi- and mononuclear complexes were almost the same both for the cation and anion, excluding those of two central carbon atoms of the bridging ligand of **1**, C(51) and C(51*).

The above data imply that these two complexes are very suitable compounds to investigate the effect of the bridging ligand on the SCO properties. As shown in Figs. 1 and 2, both complexes have intermolecular weak π–π stacking between salicylidene moieties of the adjacent molecules. Taking into this π–π stacking, **1** is considered as a quasi-one-dimensional species, whereas **2** is considered as a quasi binuclear species, including π–π stacking.

The molecular structures of the cationic parts of bi- and mononuclear complexes are shown in Figs. 3 and 4, respectively, together with the selected atom numbering scheme,

Published on the web December 13, 2007; doi:10.1246/bcsj.80.2375

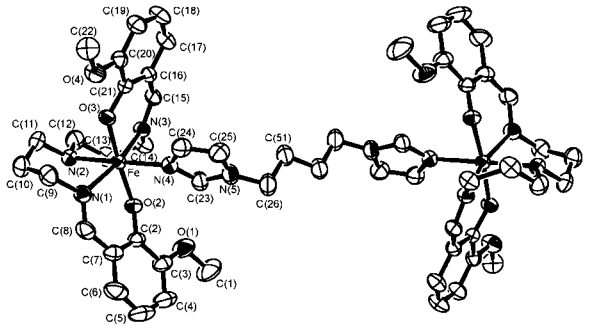

Fig. 3. Molecular structure of the cationic part of **1** at 296 K with the atoms numbering scheme.

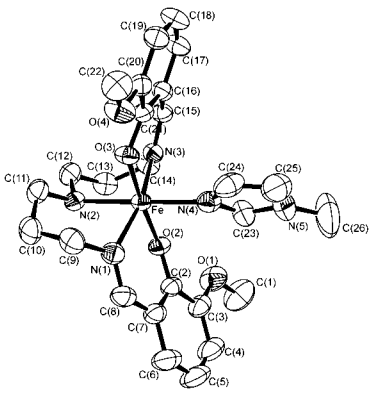

Fig. 4. Molecular structure of the cationic part of **2** at 296 K with the selected atoms numbering scheme.

where the same atom numberings are taken for these two complexes. Each Fe^{III} ion of the bi- and mononuclear complexes has a pseudo-octahedral coordination environment with N_3O_2 donor atoms of a pentadentate ligand L and N donor atom of imidazole nitrogen atom. The equatorial coordination plane consists of N_2O_2 donor atoms of the bis(3-methoxysalicylidene) moiety of the pentadentate ligand in the *trans*-form.

The magnetic susceptibilities of the crystalline samples of **1** and **2** were measured in the temperature range of 5–300 K at a 5 K min^{-1} sweeping rate under a 0.5 T applied magnetic field. The samples were quickly cooled from room temperature to 5 K within 5 s, and the magnetic susceptibilities were first measured in the warming mode from 5 to 300 K, measured in the cooling mode from 300 to 5 K.

$\chi_M T$ per Fe vs. T plots of **1** for the warming and cooling modes are shown in Fig. 5, where χ_M is the magnetic susceptibility per Fe and T is the absolute temperature. The $\chi_M T$ value in the higher temperature region of 300–150 K is constant around 3.7 cm^3 K mol^{-1}, of which the value is slightly lower than the spin-only value (4.35 cm^3 K mol^{-1}) of HS Fe^{III} species ($S = 5/2$). In the lower temperature region of 50–5 K, the $\chi_M T$ value is nearly constant at ca. 0.70 cm^3 K mol^{-1}, being compatible with the spin-only value (0.35 cm^3 K mol^{-1}) of LS Fe^{III} ($S = 1/2$). Upon lowering the temperature from 150 to 50 K, the $\chi_M T$ vs. T curve showed a two-step SCO behavior, as demonstrated by the calculation of the first derivative $\delta\chi_M T/\delta T$ in the inset of Fig. 5. The first and second SCO transitions occurred around 60 and 90 K, respectively, and the second SCO transition around 90 K is more abrupt than the first one.

$\chi_M T$ per Fe vs. T plots for **2** are shown in Fig. 6, showing

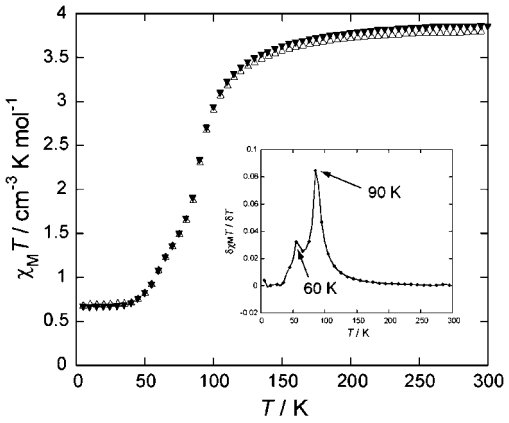

Fig. 5. $\chi_M T$ per Fe vs. T plots of **1** in the warming (△) and cooling (▼) modes. The inset represents $\delta\chi_M T/\delta T$.

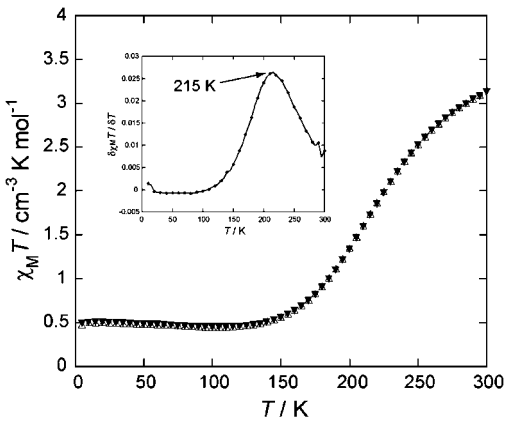

Fig. 6. $\chi_M T$ per Fe vs. T plots of **2** in the warming (△) and cooling (▼) modes. The inset represents $\delta\chi_M T/\delta T$.

no difference in the cooling and warming modes and a one-step SCO between the HS and LS states. At 5 K, the $\chi_M T$ value of 0.58 cm^3 K mol^{-1} is compatible with the spin-only value (0.35 cm^3 K mol^{-1}) of LS Fe^{III} species ($S = 1/2$). In the temperature region from 5 to 150 K, the $\chi_M T$ value was nearly constant. Upon elevating the temperature from 150 K, the $\chi_M T$ value increased gradually and monotonically from 0.58 cm^3 K mol^{-1} at 150 K to 3.13 cm^3 K mol^{-1} at 300 K. At 300 K which was the highest temperature used, the $\chi_M T$ value of 3.13 cm^3 K mol^{-1} is considerably lower than the expected value of 4.35 cm^3 K mol^{-1} for the spin-only value of HS Fe^{III} species ($S = 5/2$), indicating that a higher temperature is needed to reach the HS state. The inflection point was calculated to be $T_{1/2} = 215$ K.

Since SCO behavior was observed during the magnetic susceptibility measurements, the crystal structural studies at the lower temperature 100 K were carried out. The unit cell volume decreased from 296 to 100 K by 4.5 and 4.6% for **1** and **2**, respectively, whereas the space group did not change, indicating no phase transition during the spin transition. Table 1 shows the relevant bond distances and angles of the two complexes at 296 and 100 K. At 296 K, the average bond distances of **1** ($\langle$Fe–O$\rangle$ = 1.914 Å; $\langle$Fe–N$\rangle$ = 2.116 Å) are compatible with the reported values for the HS complexes with the same donor atoms. At 100 K, the average bond distances are $\langle$Fe–O$\rangle$ = 1.869 Å and $\langle$Fe–N$\rangle$ = 1.981 Å respectively, dem-

Table 1. Bond Distances (Å) for **1** and **2** at 296 and 100 K

Complexes	$[Fe^{III}_2L_2(bimb)](BPh_4)_2$		$[Fe^{III}L(meim)]BPh_4$	
	296 K	100 K	296 K	100 K
Fe–O(2)	1.919(2)	1.877(1)	1.910(2)	1.880(2)
Fe–O(3)	1.908(2)	1.861(1)	1.900(2)	1.863(2)
Fe–O(average)	1.914	1.869	1.905	1.872
Fe–N(1)	2.074(2)	1.971(1)	2.067(2)	1.954(2)
Fe–N(2)	2.196(2)	2.015(2)	2.176(2)	2.023(2)
Fe–N(3)	2.070(2)	1.946(1)	2.053(2)	1.946(2)
Fe–N(4)	2.124(2)	1.990(1)	2.098(2)	1.982(2)
Fe–N(average)	2.116	1.981	2.099	1.976

onstrating that the complex is almost in a LS state. At 296 K, the average bond distances of **2** ($\langle$Fe–O$\rangle$ = 1.905 Å, $\langle$Fe–N$\rangle$ = 2.099 Å) are a little shorter than those of **1**, which is consistent with the result from the magnetic measurement that **2** is between HS and LS states at 296 K. At 100 K, the average bond distances of ($\langle$Fe–O$\rangle$ = 1.872 Å and $\langle$Fe–N$\rangle$ = 1.976 Å) are compatible with the values expected for the LS complex.

Isomorphous bi- and mononuclear iron(III) complexes **1** and **2** were synthesized **1** showed a two-step spin-crossover (SCO) behavior with $T_{1/2} = 60$ and 90 K, and **2** showed a one-step SCO behavior at $T_{1/2} = 215$ K. The different SCO behavior can be ascribed to the one-dimensional structure constructed by π–π stacking and the binuclear structure.

Experimental

Preparation. The precursor complex $[Fe^{III}ClL]$ was prepared according to the method reported previously.[4a]

$[Fe^{III}_2L_2(bimb)](BPh_4)_2$ (**1**): To a solution of $[Fe^{III}ClL]$ (196 mg, 0.4 mmol) in 30 mL of methanol was added a solution of 1,4-bisimidazolylbutane dihydrate (44 mg, 0.2 mmol) in 10 mL of methanol. The mixture was warmed under stirring for 10 min and then filtered. The filtrate was added to a solution of sodium tetraphenylborate (137 mg, 0.4 mmol) in 30 mL of methanol. The resulting solution was allowed to stand for overnight, during which time black block crystals precipitated. They were collected by suction filtration, washed with methanol and dried. Anal. Calcd for $C_{102}H_{108}N_{10}O_8Fe_2B_2 \cdot H_2O \cdot CH_3OH$: C, 69.29; H, 6.44; N, 7.85%. Found: C, 69.32; H, 6.61; N, 8.16%. IR (KBr): $\nu_{C=N}$ (imine), 1614 cm^{-1}; ν_{B-C} (BPh_4^-) 733, 708 cm^{-1}.

$[Fe^{III}L(meim)]BPh_4$ (**2**): To a solution of $[Fe^{III}ClL]$ (196 mg, 0.4 mmol) in 30 mL of methanol was added a solution of *N*-methylimidazole (33 mg, 0.4 mmol) in 10 mL of methanol. The mixture was warmed and stirred for 10 min and then filtered. The filtrate was added to a solution of sodium tetraphenylborate (137 mg, 0.4 mmol) in 30 mL of methanol. The resulting solution was kept to stand for overnight, during which time black block crystals precipitated. Anal. Calcd for $C_{50}H_{53}N_5O_4FeB$: C, 70.26; H, 6.25; N, 8.19%. Found: C, 70.53; H, 6.34; N, 8.45%. IR (KBr): $\nu_{C=N}$ (imine), 1614 cm^{-1}; ν_{B-C} (BPh_4^-) 734, 708 cm^{-1}.

Physical Measurements. Elemental C, H, and N analyses were carried out by Miss. Kikue Nishiyama at the Center for Instrumental Analysis of Kumamoto University. Infrared spectra were recorded on a Nicolet Avatar 370 DTGS (Thermo Electron Corporation) spectrometer using KBr disks at ambient temperature. Magnetic susceptibilities were measured using a MPMS-5S SQUID (Quantum Design) in the 5–300 K temperature range under an applied magnetic field of 0.5 T. Corrections for diamagnetism were applied using Pascal's constants.

X-ray Crystallography. The X-ray diffraction data were collected using a Rigaku R-Axis Rapid diffractometer at 296, and 100 K. Hydrogen atoms were fixed at calculated positions and refined using a riding model. All calculations were performed using the CrystalStructure software package. Crystallographic data for $[Fe^{III}_2L_2(bimb)](BPh_4)_2$ (**1**) at 296 K: formula; $C_{102}H_{108}N_{10}O_8Fe_2B_2$, fw; 1735.35, triclinic, space group $P\bar{1}$ (No. 2), a = 12.151(4), b = 12.449(5), c = 17.195(7) Å, α = 78.72(2), β = 70.51(2), γ = 68.77(2)°, V = 2277(1) $Å^3$, Z = 1, D_{calcd} = 1.265 g cm^{-1}, μ(Mo Kα) = 3.812 cm^{-1}, R = 0.0527, R_w = 0.1354. Crystallographic data at 100 K: triclinic, space group $P\bar{1}$ (No. 2), a = 12.052(4), b = 12.245(5), c = 17.027(7) Å, α = 77.94(2), β = 69.50(2), γ = 68.14(2)°, V = 2175(1) $Å^3$, Z = 1, D_{calcd} = 1.325 g cm^{-1}, μ(Mo Kα) = 3.991 cm^{-1}, R = 0.0400, R_w = 0.1150.

Crystallographic data for $[Fe^{III}L(meim)]BPh_4$ (**2**) at 296 K: formula; $C_{50}H_{53}N_5O_4FeB$, fw; 854.66, triclinic, space group $P\bar{1}$ (No. 2), a = 12.227(3), b = 12.391(5), c = 17.204(6) Å, α = 78.23(1), β = 70.65(1), γ = 68.71(1)°, V = 2281(1) $Å^3$, Z = 2, D_{calcd} = 1.244 g cm^{-1}, μ(Mo Kα) = 3.795 cm^{-1}, R = 0.0526, R_w = 0.1314. Crystallographic data at 100 K: triclinic, space group $P\bar{1}$ (No. 2), a = 12.048(4), b = 12.213(3), c = 17.041(6) Å, α = 77.69(1), β = 69.71(1), γ = 68.27(1)°, V = 2175(1) $Å^3$, Z = 2, D_{calcd} = 1.305 g cm^{-1}, μ(Mo Kα) = 3.981 cm^{-1}, R = 0.0671, R_w = 0.1753. Crystallographic data in CIF format has been deposited at the deposition numbers 658811–658814 of CCDC.

This work was supported by a Grant-in-Aid for Science Research (No. 16205010) from the Ministry of Education, Culture, Sports, Science and Technology, Japan.

References

1 P. Gütlich, H. A. Goodwin, *Spin Crossover in Transition Metal Compounds* in *Topics in Current Chemistry* ed. by P. Gütlich, H. A. Goodwin, Topics in Current Chemistry, **2004**, Vol. 233, p. 1.

2 O. Kahn, C. J. Martinez, *Science* **1998**, *279*, 44.

3 a) S. Hayami, Z. Gu, M. Shiro, A. Einaga, A. Fujishima, O. Sato, *J. Am. Chem. Soc.* **2000**, *122*, 7126. b) Y. Sunatsuki, Y. Ikuta, N. Matsumoto, M. Kojima, S. Iijima, S. Hayami, Y. Maeda, S. Kaizaki, F. Dahan, J. P. Tuchagues, *Angew. Chem., Int. Ed.* **2003**, *42*, 1614. c) Y. Ikuta, M. Ooidemizu, Y. Yamada, S. Osa, N. Matsumoto, S. Iijima, Y. Sunatsuki, M. Kojima, F. Daha, J.-P. Tuchagues, *Inorg. Chem.* **2003**, *42*, 7001. d) H. Hagiwara, S. Hashimoto, N. Matsumoto, S. Iijima, *Inorg. Chem.* **2007**, *46*, 3136. e) M. Yamada, H. Hagiwara, H. Torigoe, N. Matsumoto, M. Kojima, F. Dahan, J. P. Tuchagues, N. Re, S. Iijima, *Chem. Eur. J.* **2006**, *12*, 4536.

4 a) N. Matsumoto, S. Ohta, C. Yoshimura, S. Kohata, Y. Maeda, H. Okawa, A. Ohyoshi, *J. Chem. Soc., Dalton Trans.* **1985**, 2575. b) S. Ohta, C. Yoshimura, N. Matsumoto, H. Okawa, A. Ohyoshi, *Bull. Chem. Soc. Jpn.* **1986**, *59*, 155. c) K. Tanimura, R. Kitashima, N. Bréfuel, M. Nakamura, N. Matsumoto, S. Shova, J.-P. Tuchagues, *Bull. Chem. Soc. Jpn.* **2005**, *78*, 1279. d) R. Kitashima, S. Imatomi, M. Yamada, N. Matsumoto, Y. Maeda, *Chem. Lett.* **2005**, *34*, 1388. e) S. Imatomi, R. Kitashima, T. Hamamatsu, M. Okeda, Y. Ogawa, N. Matsumoto, *Chem. Lett.* **2006**, *35*, 502.

5 a) R. Boča, Y. Fukuda, M. Gembický, R. Herchel, R. Jaroščiak, W. Linert, F. Renz, J. Yuzurihara, *Chem. Phys. Lett.* **2000**, *325*, 411. b) S. Hayami, Y. Hosokoshi, K. Inoue, Y. Einaga, O. Sato, Y. Maeda, *Bull. Chem. Soc. Jpn.* **2001**, *74*, 2361.